signal at $g = 2.02$ ([3Fe-4S]$^+$). This indicates that the [4Fe-4S]$^{3+}$ center is only slowly oxidized by O_2 into [3Fe-4S]$^+$ and that, were it an intermediate in scheme C, it should have been observable.

Further evidence for the formation of a 3Fe center with these type II oxidants has been recently provided by oxidizing $[Fe_4S_4(Stibt)_4]^{2-}$ (by O_2 or $[Fe(CN)_6]^{3-}$) in the presence of an equimolar amount of $CoCl_2$. A [3Fe,Co-4S]$^{2+}$ species is then formed,[32] which suggests that the Co^{2+} has been incorporated into the vacant site of a Fe_3S_4 core.

When a H_2O_2 oxidation (scheme D, Figure 3) is performed in DMF/H_2O (4/1), no formation of either [4Fe-4S]$^{3+}$, [3Fe-4S]$^+$, or Fe^{3+} is observed, and only the immediate formation of the same unidentified radical is observed ($g = 2.051$, 2.005, 1.984) up to 60 K (it power-saturates easily at low temperatures and remains stable for approximately 24 h). We were unable to determine whether [4Fe-4S]$^{3+}$ and [3Fe-4S]$^+$ are intermediates of reaction or not, since oxidation by H_2O_2 of the monooxidized cluster $[Fe_4S_4(Stibt)_4]^-$ under the same conditions immediately produced the same radical. The mechanism of action of H_2O_2 as an oxidant has been extensively investigated,[28a,33] and it is assumed therefrom that H_2O_2 oxidizes coordinated thiols via nucleophilic attack of the sulfurs on the O–O bond. The radical observed here could indeed correspond to an oxidized state of the Stibt ligands. Indeed, an EPR signal with similar g values (2.09, 2.01, 1.98) has been reported in the $[Fe(CN)_6]^{3-}$ oxidation of *A. vinelandii* FdI[6] and tentatively attributed to a cysteinyl disulfide radical. The latter has been identified among the products of radiation damage in γ-irradiated cysteine hydrochloride.[34] Its EPR spectrum is also observable at liquid-N_2 temperature, with g values of 2.06, 2.02, and 2.00, not unlike those observed here.

In conclusion, chemical oxidation of an Fe-S cluster with bulky thiolates such as $[Fe_4S_4(Stibt)_4]^{2-}$ can lead to different products when the oxidizing power and the physical properties of the reaction medium are varied:

(A) Moderate oxidants (Ag^+, I_2, $[Fe(CN)_6]^{3-}$, $[C(C_6H_5)_3]^+$) in aprotic media (CH_2Cl_2, CH_3CN) produce a one-electron metal-based oxidation, and [4Fe-4S]$^{3+}$ is quantitatively generated (type I oxidants). An increase of basicity of the solvent will also lead to an increased instability of the Fe-S core.[25]

(B) When the same moderate oxidants (Ag^+, $[Fe(CN)_6]^{3-}$) are used in a medium where H_2O is also present, an overall two-electron oxidation occurs, a 4Fe → 3Fe core conversion is then observed, and [3Fe-4S]$^+$ is generated (type II oxidants). The latter is unstable, which possibly accounts for its low concentration (less than 15%).

(C) With a stronger oxidant (oxygen) and in aprotic media (CH_2Cl_2, CH_3CN, DMF), the same 4Fe → 3Fe conversion is observed (type II oxidant). The presence of H_2O is not required, and the mechanism of oxidative conversion is possibly different from case B).

(D) Oxidation by an even stronger oxidant (H_2O_2) leads to an immediate oxidation into a radical of possibly organic nature (type III oxidant).

It appears thus that the site of oxidation on the $[Fe_4S_4(Stibt)_4]^{2-}$ cluster can be controlled by a combination of factors, principally the oxidizing strength of the oxidant and the presence of H_2O in the reaction medium. These observations may help to explain why, upon oxidation of a 4Fe protein by $[Fe(CN)_6]^{3-}$, there is either formation of a [4Fe-4S]$^{3+}$ center, conversion into a 3Fe center, or appearance of an organic radical. In the case of proteins, the medium, as well as the oxidizing strength of $[Fe(CN)_6]^{3-}$, is constant. Modulation of the reaction outcome can therefore be brought about by (1) the Fe-S cluster redox potential (the higher it is, the more stable the core with respect to oxidative degradation and the less likely a 4Fe → 3Fe conversion) and (2) the local environment of the 4Fe cluster, that is its degree of hydrophobicity and polarity (the more accessible the 4Fe cluster to water, the more easily it will destabilize and convert into a 3Fe center or even a more oxidized radical). Indeed, when characteristic features of the cluster-binding cavities in HP and in bacterial ferredoxins[2] are compared, it appears that nonpolar side chains surrounding the ferredoxin clusters differ from those found in contact with the HP cluster. Thus, the ferredoxin cavities contain mostly aliphatic chains, while the HP environment includes many aromatic side chains, and whereas the latter will effectively prevent access of solvent molecules, the ferredoxin clusters will be only moderately protected.

(32) Roth, E. K. H.; Greneche, J. M.; Jordanov, J. *J. Chem. Soc., Chem. Commun.* **1991**, 105.
(33) (a) Allison, W. S. *Acc. Chem. Res.* **1976**, *9*, 293. (b) Herting, D. L.; Sloan, C. P.; Cabral, A. W.; Krueger, J. H. *Inorg. Chem.* **1978**, *17*, 1649. (c) Adzamli, I. K.; Libson, K.; Lydon, J. D.; Elder, R. C.; Deutsch, E. *Inorg. Chem.* **1979**, *18*, 303. (d) Heeg, M. J.; Elder, R. C.; Deutsch, E. *Inorg. Chem.* **1979**, *18*, 2036.
(34) Gordy, W. In *Theory and Applications of Electron Spin Resonance*; Wiley: New York, 1980; Chapters 6 and 7.

Contribution from the School of Chemical Sciences, University of Illinois at Urbana-Champaign, 505 South Mathews Avenue, Urbana, Illinois 61801

Carbon-13 Nuclear Magnetic Resonance Spectroscopic Study of $Fe_3(CO)_{12}$ and $Ru_3(CO)_{12}$ Supported on Metal Oxide Surfaces†

Linda Reven and Eric Oldfield*

Received April 23, 1991

^{13}C-enriched $Fe_3(CO)_{12}$ and $Ru_3(CO)_{12}$ supported on a variety of metal oxide surfaces (γ-Al_2O_3, SiO_2, MgO, and HNa-Y zeolite) have been examined by carbon-13 "magic-angle" sample-spinning (MAS) nuclear magnetic resonance (NMR) spectroscopy. Our results show that the γ-Al_2O_3-supported $Fe_3(CO)_{12}$ cluster is fluxional at room temperature, but low-temperature spectra give no evidence in favor of the unusual bridging carbonyl proposed previously by some workers from infrared (IR) spectroscopy. On HNa-Y, $Fe_3(CO)_{12}$ forms a highly mobile chemisorbed species, and the ^{13}C chemical shift is consistent with formation of the dianion $[Fe_3(CO)_{11}]^{2-}$. For $Ru_3(CO)_{12}$ on γ-Al_2O_3 and SiO_2 surfaces, our results are in agreement with IR studies and show that, under anaerobic conditions, highly mobile physisorbed clusters are initially formed. Upon exposure to air or upon thermal activation, divalent tricarbonyl species are generated. The resonances of these chemisorbed species are enhanced by cross polarization and display large chemical shift anisotropies, due to restricted mobility. On MgO, $Ru_3(CO)_{12}$ behaves quite differently, the ^{13}C NMR results being consistent with the formation of highly fluxional hexaruthenium carbonyl clusters.

Introduction

Metal carbonyl clusters supported on high surface area metal oxides are of interest in relation to the cluster–surface analogy between catalytic transition-metal surfaces and molecular metal clusters,[1] as well as being good candidates for extending the study of molecular mobility to species chemisorbed on surfaces.[2-5] Not

† This work was supported by the Solid-State Chemistry Program of the U.S. National Science Foundation (Grant DMR 88-14789).

(1) Muetterties, E. L.; Rhodin, T. N.; Band, E.; Brucker, C. F.; Pretzer, W. R. *Chem. Rev.* **1979**, *79*, 91.

0020-1669/92/1331-0243$03.00/0

only do metal oxide supported metal carbonyl clusters serve as precursors in the preparation of highly dispersed metal catalysts, but they can also be novel catalysts by themselves, and many of these materials exhibit a high selectivity for specific reactions. For example, one of the heterogeneous catalysts in this study, $Fe_3(CO)_{12}$ supported on alumina, is a catalyst for the reduction of nitrobenzene to aniline, as well as a precursor for small metal aggregates which catalyze the Fisher–Tropsch reaction.[6]

One goal in the preparation of highly dispersed metal catalysts is to achieve dispersion of species of well-defined nuclearity and composition. However, the chemisorption of metal carbonyl clusters is a complicated process, the conditions under which clusters remain intact and the nature of surface bonding being poorly understood. Since many structural questions remain after characterization with more traditional methods, such as infrared and ultraviolet–visible spectroscopies and temperature-programmed desorption, other techniques—such as solid-state nuclear magnetic resonance (NMR) spectroscopy and extended X-ray adsorption fine structure (EXAFS) spectroscopy—are currently under development. For the study of dynamic processes on surfaces, there has not been an experimental probe comparable to NMR spectroscopy to determine the nature of ligand mobility in metal clusters. Surface diffusion of gases adsorbed on transition-metal surfaces can be studied by field ion spectroscopy, but this technique cannot provide the type of detailed structural information obtainable (at least in principle) from NMR spectroscopy.[1]

In the first solid-state ^{13}C NMR studies of metal clusters adsorbed on metal oxide surfaces,[7,8] only the highly mobile physisorbed species were observed. In physisorption, there are only weak van der Waals type interactions between the carbonyls and the metal oxide surface, the surface species maintaining the same basic structures and chemical shifts as in solution. In chemisorption, a covalent bond is formed between the surface and the adsorbate, and the mobility of the adsorbate becomes restricted, giving rise to an anisotropic chemical shift which broadens the resonance. Fortunately, solid-state NMR techniques, such as "magic-angle" sample spinning (MAS) and cross polarization (CP), have been used to successfully detect these less mobile chemisorbed surface species, and the reader is referred to a variety of interesting recent publications which discuss the NMR spectroscopy of supported metal carbonyls and other organometallic species, as well as model compounds, for an up-to-date account of progress in this area.[9] In this study, we describe the ^{13}C MAS NMR behavior of $Fe_3(CO)_{12}$ and $Ru_3(CO)_{12}$ adsorbed onto a variety of metal oxide surfaces. The surface chemistry and mobility of the supported (physisorbed or chemisorbed) metal carbonyl clusters are compared with their spectroscopic behavior in solution, and in addition, our results are compared with those obtained by previous workers who used other spectroscopic techniques.

Experimental Section

Chemical Aspects. $Fe_3(CO)_{12}$ (Aldrich, Milwaukee, WI) was enriched in ^{13}C by exchange with 99%-^{13}C ^{13}CO (Monsanto Research Corp., Miamisburg, OH) in heptane, and the enriched sample was then recrystallized from toluene. Three enrichment cycles with ^{13}CO, each 7 days long at room temperature, were used to obtain the high-enrichment levels (typically ~60% ^{13}C) needed for surface studies. $Ru_3(CO)_{12}$ (Strem Chemicals, Newbury Port, MA) was dissolved in heptane and ^{13}CO exchange carried out at 80 °C for 8 h, the product being recrystallized from 1,2-dichloroethane. Samples were examined by solution ^{13}C NMR spectroscopy to verify both purity and uniformity of enrichment. Overall enrichment levels were determined by electron impact mass spectroscopy.

Support Preparations. γ-Al_2O_3 (surface area ca. 200 m^2/g) was derived from Catapal boehmite (Conoco Chemicals, Houston, TX) by calcining at 650 °C for 8 h. Silica (surface area ca. 220 m^2/g) was Cab-O-Sil M5 (Cabot Corporation, Tuscola, IL) which was dried at 100 °C under vacuum to remove adsorbed water. MgO (surface area ca. 180 m^2/g) was derived by decomposing $Mg(OH)_2$ under vacuum at 400 °C for 2 h. Linde HNa–Y zeolite (SK40, Alfa, Danvers, MA) was used without pretreatment. Surface area measurements of the supports were performed on an AUTOSORB-1 BET instrument (Quantachrome Corp., Syosset, NY).

$[Me_4N][HFe_3(CO)_{11}]$ was prepared from $Fe_3(CO)_{12}$ as described by Hieber and Brendel.[10] A 1.68-g sample of KOH and 15 mL of CH_3OH were combined in a Schlenk tube, which was then degassed by using three freeze–pump–thaw cycles. An 0.8155-g amount of $Fe_3(CO)_{12}$ was added to the KOH/CH_3OH solution under an argon atmosphere, and the mixture was stirred. After a few minutes, the solution turned reddish brown and was then transferred, along with 35 mL of degassed glacial acetic acid, into a Schlenk filter flask, using a gastight syringe. The solution was filtered into a Schlenk round-bottomed flask containing a degassed solution of 0.5 g of $[(CH_3)_4N]I$ in 30 mL of distilled water. The bright red crystals which formed were filtered out, washed with water, and then dried under vacuum. $[Me_4N][HFe_3(CO)_{11}]$ was enriched in ^{13}C by stirring a dichloroethane solution under ^{13}CO at room temperature for 23 days, and the product was then recrystallized from 1-propanol.

$Fe_3(CO)_{12}/\gamma$-Al_2O_3 samples were prepared using Schlenk techniques by impregnating hydroxylated γ-Al_2O_3 (surface area ca. 200 m^2/g) with a hexane solution of 60% ^{13}C-enriched $Fe_3(CO)_{12}$, to give loadings of between 2 and 5 wt % metal carbonyl. Hexane was dried over CaH_2 and then distilled just prior to use. When a solution of $Fe_3(CO)_{12}$ in hexane was added to the γ-Al_2O_3, the solution decolorized, and the alumina became dark red. The sample was washed several times with hexane, the solvent syringed off, and the sample dried under a stream of argon. Infrared analysis of a representative sample (Nujol mull) revealed strong absorptions at ~2006 and 1986 cm^{-1} and a weaker, broad absorption at ~1645 cm^{-1} (data not shown), in accord with the results of Hanson et al.[23]

$Fe_3(CO)_{12}$/HNa–Y zeolite was prepared basically according to Iwamoto et al.[11] except that the ^{13}C-enriched $Fe_3(CO)_{12}$ was first dissolved in hexane and the solution then mixed with the zeolite in order to achieve a higher loading. A 43.7-mg sample of $[^{13}C]Fe_3(CO)_{12}$ in degassed hexane was added to 0.6747 g of Linde HNa–Y zeolite under an argon atmosphere. $Fe_3(CO)_{12}$ did not immediately adsorb from solution onto the zeolite, as occurred with γ-Al_2O_3. The hexane was thus pumped off, and the finely mixed zeolite and $Fe_3(CO)_{12}$ were placed under an argon atmosphere, then warmed to 70 °C for 8 h, and evacuated at the same temperature for 1 h to remove any unreacted $Fe_3(CO)_{12}$.

$(\mu$-H)$Ru_3(CO)_{10}(SC_2H_5)$ was prepared from $Ru_3(CO)_{12}$ and ethanethiol according to the procedure described by Crooks et al.[12] A 0.2-mL portion of ethanethiol (Aldrich, Milwaukee, WI) was added to a solution of 100 mL of benzene and 1.0 g of $Ru_3(CO)_{12}$ under argon; the mixture was then refluxed for 15 min. After cooling, the solvent was pumped off, leaving a dark orange oil, which was crystallized from pentane, producing dark orange crystals, which were characterized by infrared spectroscopy. For ^{13}C enrichment, a solution of $(\mu$-H)$Ru_3(CO)_{10}(SC_2H_5)$ in hexane was warmed to 40 °C and stirred under ^{13}CO for 5 days.

$[Ru(CO)_3Cl_2]_2$ was prepared from 75% ^{13}C-enriched $Ru_3(CO)_{12}$.[13] A 0.57-g sample of $Ru_3(CO)_{12}$ was dissolved in 40 mL of chloroform in a glass-lined autoclave. The autoclave was charged with 5 atm of N_2 and heated to 110 °C in an oil bath for 8 h. The autoclave was vented and

(2) Yermakov, Yu. I.; Kuznetsov, B. N.; Zakharov, V. A. *Catalysis by Supported Metal Complexes*; Elsevier: Amsterdam, 1981.
(3) Hartley, F. R. *Supported Metal Complexes*; Reidel: Dordrecht, The Netherlands, 1985.
(4) *Metal Clusters in Catalysis*; Gates, B. C., Guczi, L., Knözinger, H., Eds.; Elsevier: Amsterdam, 1986.
(5) *Surface Organometallic Chemistry: Molecular Approach to Surface Catalysis*; Basset, J. M., et al., Eds.; Kluwer Academic Publishers: Dordrecht, The Netherlands, 1988.
(6) NGuini Effa, J. B.; Djebailli, B.; Lieto, J.; Aune, J. P. *J. Chem. Soc., Chem. Commun.* **1983**, 408.
(7) Ben-Taarit, Y.; Wicker, G.; Naccache, C. In *Magnetic Resonance in Colloid and Interface Science*; Fraissard, J. P., Resing, H. A., Eds.; Reidel: Dordrecht, The Netherlands, 1980; p 497.
(8) Derouane, E. G.; Nagy, J. B.; Védrine, J. C. *J. Catal.* **1977**, *46*, 434.
(9) Hasselbring, L.; Puga, J.; Dybowski, C.; Gates, B. C. *J. Phys. Chem.* **1988**, *92*, 3934. Lamb, H. H.; Hasselbring, L. C.; Dybowski, C.; Gates, B. C. *J. Mol. Catal.* **1989**, *56*, 36. Toscano, P. J.; Marks, T. J. *Langmuir* **1986**, *2*, 820. Heddon, D.; Marks, T. J. *J. Am. Chem. Soc.* **1988**, *110*, 1647. Finch, W. C.; Gillespie, R. D.; Heddon, D.; Marks, T. J. *J. Am. Chem. Soc.* **1990**, *112*, 6221. Uchiyama, S.; Gates, B. C. *J. Catal.* **1988**, *110*, 388. Puga, J.; Fehlner, T. P.; Gates, B. C.; Braga, D.; Grepioni, F. *Inorg. Chem.* **1990**, *29*, 2376.
(10) Hieber, W.; Brendel, G. Z. *Z. Anorg. Allg. Chem.* **1957**, *289*, 324.
(11) Iwamoto, M.; Nakamura, S.; Kusano, H.; Kagawa, S. *J. Phys. Chem.* **1986**, *90*, 5244.
(12) Crooks, G. R.; Johnson, B. F. G.; Lewis, J.; Williams, I. G. *J. Chem. Soc. A* **1969**, 797.
(13) Mantovani, A.; Cenini, S. *Inorg. Synth.* **1976**, *16*, 51.

Table I. Comparison between Methods Used To Prepare Supported Metal Carbonyls

ref	wt % metal carbonyl	support treatments	surface area, m^2/g
		$Ru_3(CO)_{12}/\gamma\text{-}Al_2O_3$	
this work	~2.4	Catapal B derived by heating to 650 °C in air for 8 h; no pretreatment	200
14	0.7, 3.3	Degussa P110; no pretreatment	100
38	0.63–2.5	Kaiser 201 heated in vacuo at 100–800 °C, calcined in air at 400 °C	NR[a]
39	NR	NR	NR
		$Ru_3(CO)_{12}/SiO_2$	
this work	2.8	Cab-O-Sil M5, 20 h at 100 °C in vacuo, carbonyl-activated at 80 °C for 2 h	220
40	2–4	Aerosil O Degussa, 16 h at 25 or 225 °C in vacuo, thermally activated at 80 °C for several hours	200
		$Ru_3(CO)_{12}/MgO$	
this work	4.9	MgO from $Mg(OH)_2$, 400 °C in vacuo for 2 h	180
48	2.2	MgO from $Mg(OH)_2$, 400 °C in vacuo, several O_2 cycles at 400 °C, rehydrated, heated in vacuo at 25, 200, and 500 °C	200
16	0.95	MgO heated in vacuo at 100 °C	29
		$Fe_3(CO)_{12}/\gamma\text{-}Al_2O_3$	
this work	2–5	Catapal B $\gamma\text{-}Al_2O_3$	200
20	5–6	Degussa $\gamma\text{-}Al_2O_3$, 500 °C O_2 cycle, rehydrated at 25 °C	100
23	NR	Catapal SB, 400 °C O_2 cycle, hydrated at 100 °C	NR
22	NR	$\gamma\text{-}Al_2O_3$ heated in dry air at 300 °C for 2 h	150
		$Fe_3(CO)_{12}$/HNa–Y Zeolite	
this work	6.1	SK-40 zeolite, as received	NR
11	3.7	SK-40 zeolite, 400 °C O_2 cycle, rehydrated at 25 °C	NR

[a] Not reported or measured.

cooled, and the suspension of $[Ru(CO)_3Cl_2]_2$ was collected on a filter and washed with chloroform.

$Ru_3(CO)_{12}/\gamma\text{-}Al_2O_3$ was prepared from 75% ^{13}C-enriched $Ru_3(CO)_{12}$ and $\gamma\text{-}Al_2O_3$ (surface area ca. 200 m^2/g).[14] A 6.1-mg sample of $Ru_3(CO)_{12}$ in hexane was added to 0.25 g of $\gamma\text{-}Al_2O_3$ under argon and stirred. The alumina turned light yellow and was then washed with hexane to remove any possible excess $Ru_3(CO)_{12}$. The solvent was pumped off, and the sample was stored under argon.

$Ru_3(CO)_{12}/SiO_2$ was prepared from 75% ^{13}C-enriched $Ru_3(CO)_{12}$ and silica (surface area ca. 220 m^2/g).[15] A 20-mg sample of $Ru_3(CO)_{12}$ in hexane was added to 0.7 g of SiO_2, and the mixture was then stirred under argon. Excess solvent was removed, and the sample was dried under vacuum. The silica was light yellow-orange. The sample was thermally activated by heating to 80 °C for 2 h, under vacuum. The silica turned light tan after thermal activation.

$Ru_3(CO)_{12}/MgO$ was prepared from 75% ^{13}C-enriched $Ru_3(CO)_{12}$ and MgO (surface area ca. 180 m^2/g).[16] A 34.2-mg sample of $Ru_3(CO)_{12}$ in hexane was added to 0.7 g of MgO, under argon. After stirring, the solvent decolorized and the magnesia turned dark orange. The sample was then washed several times with hexane, dried under vacuum, and stored under argon.

NMR Spectroscopy. Solid-state ^{13}C NMR spectra were obtained using a "home-built" 360-MHz (8.45-T) NMR spectrometer. Solution spectra were obtained on a 500-MHz (11.7-T) instrument.[17] For MAS NMR spectroscopy, the samples were packed into 7-mm cylindrical rotors (Doty Scientific, Columbia, SC) in a glovebag, under a nitrogen atmosphere. Sample weights were typically 400 mg. All spectra were obtained using 90° pulse excitation (typically 5–10 μs), with high power (40–60 W) proton decoupling during data acquisition. In some cases, spectra were obtained under cross-polarization conditions, in order to avoid the broad Kel-F probe background or to obtain qualitative information on the presence of protons.

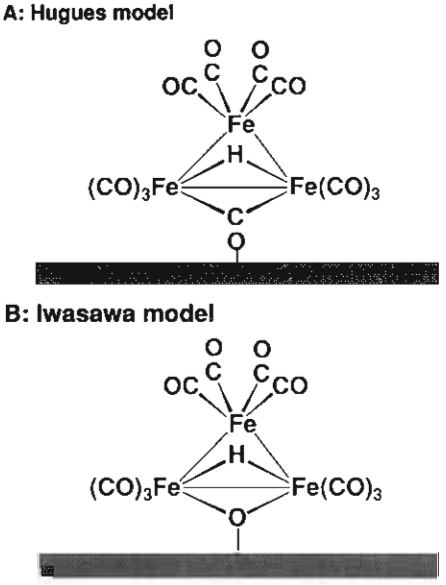

Figure 1. Proposed structures of chemisorbed $Fe_3(CO)_{12}$ on $\gamma\text{-}Al_2O_3$: (A) as proposed by Hugues et al.;[19] (B) as proposed by Iwasawa et al.[22]

Results

We have obtained ^{13}C magic-angle sample-spinning NMR spectra of a range of supported (and unsupported) metal carbonyls, and Table I shows a comparison between the support and sample preparation protocols we have used (for the supported carbonyls) with those reported by other workers. Figures 2–9 show the experimental ^{13}C NMR spectra we have recorded: Figure 2, $Fe_3(CO)_{12}/\gamma\text{-}Al_2O_3$; Figure 3, $[Me_4N][HFe_3(CO)_{11}]$; Figure 4, $Fe_3(CO)_{12}$/HNa–Y zeolite; Figure 5, $Ru_3(CO)_{12}/\gamma\text{-}Al_2O_3$; Figure 6, $Ru_3(CO)_{12}/SiO_2$; Figure 7, $HRu_3(CO)_{10}(SCH_2CH_3)$; Figure 8, $[Ru(CO)_3Cl_2]_2$; Figure 9, $Ru_3(CO)_{12}/MgO$. A compilation of the chemical shift tensor elements for iron and ruthenium carbonyl clusters is given in Table II, and carbon-13 isotropic chemical shifts for some ruthenium carbonyl clusters are presented in Table III. These will be introduced at appropriate places in the sections which follow.

Discussion

$Fe_3(CO)_{12}$ Adsorbed on $\gamma\text{-}Al_2O_3$. The reaction of $Fe_3(CO)_{12}$ with silica and hydroxylated alumina and magnesia surfaces has been studied by infrared, UV–visible, and ESR spectroscopies.[18-23] On silica, $Fe_3(CO)_{12}$ is only physisorbed and can be extracted quantitatively with *n*-hexane. However, when a hexane solution of $Fe_3(CO)_{12}$ is put into contact with hydroxylated alumina or magnesia, chemisorption takes place; the green cluster in solution transfers to the alumina or magnesia support, forming a dark pink surface species, which cannot be extracted with *n*-hexane. Hugues and co-workers propose that there is a nucleophilic surface attack on a CO ligand, with simultaneous elimination of CO_2, to form the monoanionic cluster $[HFe_3(CO)_{11}]^-$:[20]

$$Fe_3(CO)_{12}(ads) + H\text{–}O\text{–}[M] \rightarrow [HFe_3(CO)_{11}]^-[M]^+ + CO_2(ads) \quad (1)$$

(14) Zecchina, A.; Guglielminotti, E.; Bossi, A.; Camia, M. *J. Catal.* **1982**, *74*, 225.
(15) Theolier, A.; Choplin, A.; D'Ornelas, L.; Basset, J. M.; Zanderighi, G.; Ugo, R.; Psaro, R.; Sourisseau, C. *Polyhedron* **1983**, *2*, 119.
(16) Pierantozzi, R.; Valagene, E. G.; Nordquist, A. F.; Dyer, P. N. *J. Mol. Catal.* **1989**, *21*, 189.
(17) Smith, K. A.; Kirkpatrick, R. J.; Oldfield, E.; Henderson, D. M. *Am. Mineral.* **1983**, *68*, 1206.
(18) Lázár, L.; Matusek, K.; Mink, J.; Dobos, S.; Guczi, L.; Vizi-Orosz, A.; Markó, L.; Reiff, W. M. *J. Catal.* **1984**, *87*, 163.
(19) Hugues, F.; Smith, A. K.; Ben-Taarit, Y.; Basset, J. M.; Commereuc, D.; Chauvin, Y. *J. Chem. Soc., Chem. Commun.* **1980**, 68.
(20) Hugues, F.; Basset, J. M.; Ben-Taarit, Y.; Choplin, A.; Primet, M.; Rojas, D.; Smith, A. K. *J. Am. Chem. Soc.* **1982**, *104*, 7020.
(21) Hugues, F.; Dalmon, J. A.; Bussiere, P.; Smith, A. K.; Basset, J. M.; Olivier, D. *J. Phys. Chem.* **1982**, *86*, 5136.
(22) Iwasawa, Y.; Yamada, M.; Ogasawara, S.; Sato, Y.; Kuroda, H. *Chem. Lett.* **1983**, 621.
(23) Hanson, B. E.; Bergmeister, J. J., III; Petty, J. T.; Connaway, M. C. *Inorg. Chem.* **1986**, *25*, 3089. Hanson, B. E. In *Advances in Dynamic Stereochemistry*; Gielen, M. F., Ed.; Freund Publishing House Ltd.: London, 1985; Vol. 1, p 89.

Table II. Carbon-13 Chemical Shift Tensors for Iron and Ruthenium Carbonyl Clusters

compd	site	δ_i,[a] ppm	δ_{11},[b] ppm	δ_{22},[b] ppm	δ_{33},[b] ppm	$\Delta\delta$,[c] ppm	$\lvert\eta\rvert$[d]
$Fe_3(CO)_{12}$		203	342	322	−54	386	0.08
		210	344	328	−42	378	0.06
		213	348	311	−20	350	0.16
		225	328	321	26	298	0.04
	static	212	325	316	−6	327	0.04
$Ru_3(CO)_{12}$	axial	210	346	338	−54	396	0.03
	equatorial	189	330	312	−74	395	0.07
	static	201	348	319	−63	397	0.11
$[Me_4N][HFe_3(CO)_{11}]$	axial	220	382	333	−52	410	0.18
	equatorial	210	369	334	−73	425	0.12
	bridging	277	298	287	193	99	0.13
$Fe_3(CO)_{12}/\gamma$-Al_2O_3		221	405	259	36	296	0.78
$Fe_3(CO)_{12}$/HNa−Y		230	232	234	221	12	0.22
$(\mu$-H)$Ru_3(CO)_{10}(SC_2H_5)$		205	382	347	−74	438	0.13
		199	361	317	−81	420	0.16
		193	364	307	−92	428	0.20
		185	338	312	−96	421	0.09
$[Ru(CO)_3Cl_2]_2$		182	337	291	−85	400	0.17
$Ru_3(CO)_{12}/\gamma$-Al_2O_3		194	358	310	−81	417	0.17
$Ru_3(CO)_{12}/SiO_2$ (in air)		193	365	312	−91	429	0.19

[a] Isotropic chemical shift, in ppm downfield from an external standard of tetramethylsilane. [b] Chemical shift tensor element component obtained by using the graphical method of Herzfeld and Berger.[32] δ_{11} is the most deshielded tensor element; δ_{33}, the most shielded. High-frequency, low-field, paramagnetic or deshielded values are positive (IUPAC δ scale). [c] Anisotropy of the shift tensor, $\Delta\delta = \delta_{33} - {}^1/_2(\delta_{11} + \delta_{22})$. [d] Asymmetry parameter of the chemical shift tensor. The absolute value can vary from 0 to 1.

Table III. Carbon-13 Isotropic Chemical Shifts for Ruthenium Carbonyl Clusters

species	δ_i, ppm	ref
$Ru(CO)_2(OM<)$	193	this work
$Ru(CO)_3(OSi<)$	178	this work
$[Ru(CO)_3Cl_2]_2$	184.5 (2), 181.2 (1)	this work
$Ru(CO)_4I_2$	178.2, 177.8	45
$HRu_3(CO)_{12}(\mu$-OSi<)	197.7	this work
$HRu_3(CO)_{12}(SC_2H_5)$	205 (2), 199 (4), 193 (2), 185 (2)	this work
$Ru_3(CO)_{12}$	199.7	56
$[HRu_3(CO)_{11}]^-$	200.9, 202.2	50, 51
$[Ru_3(CO)_{11}]^{2-}$	215.5	51
$H_2Ru_4(CO)_{13}$	195.5	57
$[HRu_4(CO)_{13}]^-$	205	51
$[HRu_4(CO)_{12}]^{3-}$	218.1 (5), 207.6 (7)	51
$[H_2Ru_4(CO)_{12}]^{2-}$	220.3	58
$[Ru_4(CO)_{13}]^{2-}$	223.5	51
$[Ru_4(CO)_{12}]^{4-}$	227	51
$[Ru_6(CO)_{18}]^{2-}$	211	51
$[Ru_6C(CO)_{16}]^{2-}$	213 (16), 288 (1)	59
$[Ru_6(CO)_{17}]^{4-}$	228.7	53
$[Ru_6(CO)_{16}]^{6-}$	228.6	53

The anionic cluster, whose suggested structure is shown in Figure 1A, interacts with a surface Lewis acid site via the bridging CO ligand. The adsorbed anion, $[HFe_3(CO)_{11}]^-$, was characterized by infrared spectroscopy, which showed a broad weak band, assigned to the bridging carbonyl, at 1590 cm^{-1}. This is much lower than observed in solution for the anionic species. In addition, Hugues et al. extracted the metal cluster with tetraethylammonium chloride and characterized it by ^1H NMR and infrared spectroscopies. The proton chemical shift of 15 ppm and the observed IR results were in agreement with those for $[HFe_3(CO)_{11}][N(C_2H_5)_4]$.[20]

Other workers, however, have not observed the infrared bands assigned by Hugues and co-workers to the bridging carbonyl ligand. For example, Iwasawa et al.[22] used EXAFS, IR, and UV–visible spectroscopies, along with measurements of the gas evolved during chemisorption, to determine that the grafted cluster had the structure shown in Figure 1B. They proposed that this structure, which lacks a bridging carbonyl, forms through the oxidative addition of a surface hydroxyl group to an Fe–Fe bond. However, the chemisorption was performed under somewhat different reaction conditions: $Fe_3(CO)_{12}$ and γ-Al_2O_3 were dry-mixed and then heated under vacuum to 313 K for 2 h.

Hanson et al.[23] have more recently carried out an in situ study of the chemisorption of $Fe_3(CO)_{12}$ on γ-Al_2O_3 in order to try to resolve the different proposed structures of the surface species. They found a bridging carbonyl band at 1695 cm^{-1} for some γ-Al_2O_3-supported samples, but in general this band was difficult to observe. Hanson et al. proposed that the anion $[HFe_3(CO)_{11}]^-$ is initially formed but that subcarbonyls of the form $HFe_3(CO)_{11-x}$ may also be generated, with structures similar to that shown in Figure 1B. The presence of subcarbonyls having this basic structure could account for the lack of a distinct bridging carbonyl band in the infrared spectra for many such samples.

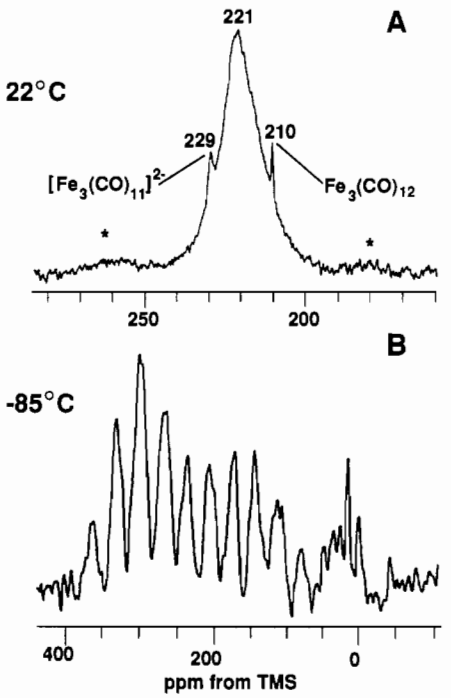

Figure 2. ^{13}C MAS NMR spectra of $Fe_3(CO)_{12}/\gamma$-Al_2O_3 at 8.45 T (90.5 MHz): (A) 22 °C, 3.5-kHz spinning speed, 900 acquisitions, 2-s recycle time; (B) −85 °C, 2.5-kHz spinning speed, 4000 acquisitions, 2-s recycle time.

The room-temperature proton-decoupled ^{13}C MAS NMR spectrum of $Fe_3(CO)_{12}/\gamma$-Al_2O_3 is shown in Figure 2A. There is a small sharp resonance at 210 ppm, an intense broad peak at 221 ppm, with small sidebands (*), and a second small peak at 229 ppm, in agreement with previous work by Hanson et al.,[23] except that our spectrum (which has a better signal-to-noise ratio)

contains the additional peak at 229 ppm. The sharp resonance at 210 ppm is assigned to physisorbed $Fe_3(CO)_{12}$, since the chemical shift is close to that observed in solution (212 ppm). For samples with loadings higher than 2 wt %, Hugues and co-workers[20] were able to extract $Fe_3(CO)_{12}$ into *n*-hexane. We observed the sharp peak, due to physisorbed $Fe_3(CO)_{12}$, in samples with loadings higher than 3 wt %, even though the samples had been washed several times with hexane. The solution-like resonance is due to rapid tumbling of the physisorbed cluster, which averages the chemical shift anisotropy to zero. Similar behavior is observed for mononuclear carbonyls, such as $Mo(CO)_6$, $Ni(CO)_4$, $Fe(CO)_5$, and $Cr(CO)_6$, adsorbed onto various oxide supports[7,8,24] as well as for $Os_3(CO)_{12}/SiO_2$ before thermal activation.[25]

The broad peak at 221 ppm in the NMR spectrum of $Fe_3(CO)_{12}/\gamma$-Al_2O_3 is assigned to a chemisorbed iron carbonyl cluster, on the basis of its chemical shift, which is identical to that of the anionic hydride $[HFe_3(CO)_{11}]^-$ in solution.[26] The fact that the shift is so close to that of the solution spectrum and the observation that the peak is relatively narrow suggest physisorption, not chemisorption. Basset and co-workers assert that the grafted cluster exists as a tight-ion-pair complex, in which the lone-pair electrons of the bridging carbonyl oxygen interact with a surface aluminum cation. They base this bonding picture on the low stretching frequency of a bridging carbonyl in the infrared spectrum. Extensive infrared studies of the anion $[HFe_3(CO)_{11}]^-$ show that the bridging carbonyl is very sensitive to counterion and solvent effects.[27-30] Likewise, the ^{13}C NMR resonance of the bridging carbonyl is found to shift downfield with increasing polarity of the solvent and may vary between 285 and 355 ppm.[26] If there exists a strong Lewis acid–base interaction between the aluminum cations and the bridging carbonyl ligand, we might expect the grafted anionic hydride to have a shift downfield from that observed in nonpolar solvents. In addition, if an unusual bridging CO is present, we might expect to be able to observe it via ^{13}C NMR spectroscopy.

Since the peak we have assigned to the supported iron carbonylate has only weak spinning sidebands, this species must be undergoing considerable motional averaging of the carbonyl ligand chemical shifts. MAS reduces the line width from 1500 to 800 Hz. The breadth of the resonance at 221 ppm is of interest and could be due to several mechanisms. First, it could be due to the presence of subcarbonyl species as proposed by Hanson et al.[23] and/or adsorption at slightly different sites, resulting in a distribution of chemical shifts. Second, it could be due to isotropic motion (or ligand exchange) at an "intermediate" rate, causing exchange broadening. Third, the presence of paramagnetic species cannot be ignored. For example, the disproportionation reactions proposed by Hanson et al. require the formation of Fe(II) species, and these workers found that sealed samples of $Fe_3(CO)_{12}/\gamma$-Al_2O_3 were slightly paramagnetic, although ESR experiments have not detected iron cations on the alumina.[23] On the basis of the results of variable-temperature NMR experiments, we favor the idea that the breadth of the peak at 221 ppm is due to anisotropic motion and/or incomplete scrambling of the carbonyl ligands. The dynamic properties of $[HFe_3(CO)_{11}]^-$ have been carefully studied in solution by variable-temperature ^{13}C NMR spectroscopy.[26] Whereas $Fe_3(CO)_{12}$ has an extremely low barrier to carbonyl ligand migration, a sharp ^{13}C NMR singlet being observed down to −150 °C,[31] the fluxional processes of $[HFe_3(CO)_{11}]^-$ cease at much higher temperatures. For example, at room temperature,

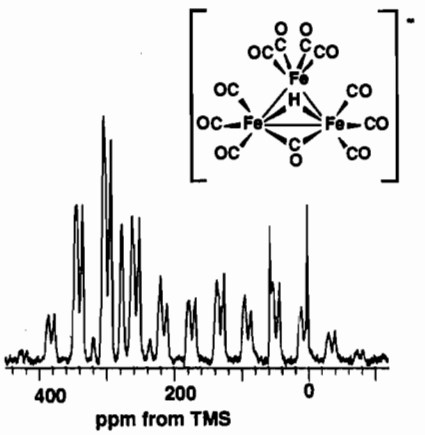

Figure 3. ^{13}C MAS NMR spectrum of $[Me_4N][HFe_3(CO)_{11}]$ at 8.45 T (90.5 MHz; 3.2-kHz spinning speed, 72 acquisitions, 60-s recycle time).

one peak (at 221 ppm) is observed,[26] but as the temperature is lowered to −30 °C, two signals (at 259.8 and 214.8 ppm), in a 1 to 10 intensity ratio are observed. The low-field peak is due to scrambling of the bridging carbonyl with one of the terminal carbonyl groups. Wilkinson and Todd[26] proposed a mechanism involving a pairwise opening and closing of the hydride and bridging carbonyl units to account for this scrambling process. At −107 °C, all the fluxional processes are frozen out, and seven separate resonances are observed.[26]

In order to determine where the bridging carbonyl resonates in the solid-state NMR spectrum of authentic $[HFe_3(CO)_{11}]^-$ and to estimate its chemical shift anisotropy, we have investigated the ^{13}C MAS spectrum of the model compound $[Me_4N][HFe_3(CO)_{11}]^-$. As may be deduced from Figure 3, $[HFe_3(CO)_{11}]^-$ in this model system is completely rigid in the solid state at room temperature, quite unlike $Fe_3(CO)_{12}$. The values for the chemical shift anisotropies (CSA) of the CO ligands, as calculated from sideband intensities using the graphical method of Herzfeld and Berger,[32] are given in Table I. The CSA values for the terminal carbonyl ligands (at 220 and 212 ppm) were found to be 410 and 425 ppm, respectively, but the bridging carbonyl (at 276.9 ppm) has an very small CSA, of only 99 ppm. If the alumina-supported monoanion has an intact bridging carbonyl ligand, it seems almost certain that it would be visible in a low-temperature MAS NMR spectrum, when the slow exchange limit is reached, since its peak height should be ≈4 times larger than that of a terminal carbonyl (≈$^1/_4$ the CSA). A ^{13}C MAS NMR spectrum of $Fe_3(CO)_{12}/\gamma$-Al_2O_3 taken at −85 °C is shown in Figure 2B. The spectrum shows a series of broad spinning sidebands, but no bridging carbonyl resonance is apparent. The broadness of the sidebands may be due to unresolved resonances of the terminal carbonyl ligands and/or the presence of residual motion. In solution, the fluxional behavior of the anion begins to cease at ∼−80 °C, where separate peaks are resolved, and the peaks become narrow at −107 °C. Another MAS NMR spectrum of $Fe_3(CO)_{12}/\gamma$-Al_2O_3, at −113 °C, also showed a similar set of broad spinning sidebands. Our results thus give no evidence for the bridging CO shown in Figure 1A and thus tend to support the structure in Figure 1B as a major contributor to the spectra shown in Figure 2. Of course, if the interaction with the presumed surface Lewis acid site were to cause a major increase in the bridging CO's CSA, then we would not expect to be able to observe it at currently achievable spectral signal-to-noise ratios. In the absence of any evidence that this actually occurs, however, our results would tend to favor the oxo-bridged species in Figure 1B—the same structure as found previously for $Os_3(CO)_{12}$ on silica[25]—as the major contributor to our spectrum.

We should add at this point that the presence of a bridging CO in $Fe_3(CO)_{12}/\gamma$-Al_2O_3 is a quite controversial point. Infrared spectra of our sample are similar to those reported by Hanson and co-workers (23), who noted that "If the 1695 cm^{-1} band *is*

(24) Shirley, W. M.; McGarvey, B. R.; Maiti, B.; Brenner, A.; Cichowlas, A. *J. Mol. Catal.* **1985**, *29*, 259.
(25) Walter, T. H.; Frauenhoff, G. R.; Shapley, J. R.; Oldfield, E. *Inorg. Chem.* **1988**, *27*, 2561.
(26) Wilkinson, J. R.; Todd, L. J. *J. Organomet. Chem.* **1976**, *118*, 199.
(27) Hodali, H. A.; Shriver, D. F.; Ammlung, C. A. *J. Am. Chem. Soc.* **1978**, *100*, 5239.
(28) Hodali, H. A.; Shriver, D. F. *Inorg. Chem.* **1979**, *18*, 1236.
(29) Chen, C. K.; Cheng, C. H. *Inorg. Chem.* **1983**, *22*, 3378.
(30) Schick, K. P.; Jones, N. L.; Sekula, P.; Boag, N. M.; Labinger, J. A.; Kaesz, H. D. *Inorg. Chem.* **1984**, *23*, 2204.
(31) Cotton, F. A.; Hunter, D. L. *Inorg. Chim. Acta* **1974**, *11*, L9.
(32) Herzfeld, J.; Berger, A. E. *J. Chem. Phys.* **1980**, *73*, 6021.

a bridging carbonyl, [then] its appearance is very sensitive to reaction conditions. In all samples in which the 1695 cm^{-1} band is observed, it is removed by evacuation of the sample....".[23] Our NMR results are thus in accord with the IR and CO evolution data of Hanson et al.[23]—but do not rule out the possibility that, prepared under slightly different reaction conditions, the complex could contain a bridging carbonyl.

In the room-temperature spectrum of $Fe_3(CO)_{12}/\gamma$-Al_2O_3 shown in Figure 2A, there is also a very small peak at 229 ppm, which is only observed at very high loadings (>4 wt %). We assign this peak to the fluxional dianion $[Fe_3(CO)_{11}]^{2-}$, which has an isotropic chemical shift of 230.7 ppm in solution.[28] In basic solution, the direct formation of the monoanion occurs according to the reaction[9]

$$Fe_3(CO)_{12} + OH^- \xrightarrow[MeOH]{KOH,\ 25\ °C} [HFe_3(CO)_{11}]^- + CO_2 \quad (2)$$

While under more basic conditions, the dianion forms:

$$Fe_3(CO)_{12} + 2OH^- \rightarrow [Fe_3(CO)_{11}]^{2-} + CO_2 + H_2O \quad (3)$$

At higher loadings, there is nearly complete coverage of the alumina surface, with most of the available hydroxyl groups having reacted with $Fe_3(CO)_{12}$,[20] and the presence of the dianionic species, which is formed under more basic conditions, seems less likely. However, deprotonation of $[HFe_3(CO)_{11}]^-$ to give the dianion is a reversible process, and the surface equilibrium may be such that at high loadings a small amount of the dianion exists.

Our ^{13}C MAS NMR results obtained with the $Fe_3(CO)_{12}/\gamma$-Al_2O_3 system thus tend to support the idea that the γ-Al_2O_3-grafted $Fe_3(CO)_{12}$ metal carbonyl cluster is highly mobile, or fluxional, at room temperature, while at lower temperatures, we have been unable to obtain, in our samples, evidence in favor of a unique bridging carbonyl ligand. If the CSA of the bridging CO were as small as that of the model compound $[Me_4N][HFe_3(CO)_{11}]$, then its relative peak height and chemical shift should make it clearly visible. On the other hand, if it were involved in some type of intermediate exchange rate process, then it could undergo additional line broadening and be more difficult to detect. The simplest explanation, however, is that the structure shown in Figure 1B is the major contributor to the spectra shown in Figure 2. This species $(\mu\text{-H})Fe_3(CO)_{10}(OAl{\equiv})$ is thus formally analogous to the Os species $(\mu\text{-H})Os_3(CO)_{10}(OSi{\equiv})$ found previously for $Os_3(CO)_{12}$ on SiO_2.[25]

$Fe_3(CO)_{12}$ on HNa–Y Zeolite. The first studies of the adsorption of iron carbonyl clusters onto zeolites involved dehydrated H–Y type zeolites. In these systems, $Fe_3(CO)_{12}$ retains its molecular structure, the zeolite takes on the green color of $Fe_3(CO)_{12}$, and no CO evolution is observed. Iwamoto et al.[10] studied the reactions of $Fe(CO)_5$, $Fe_2(CO)_9$, and $Fe_3(CO)_{12}$ with hydroxylated Na–Y zeolites. When $Fe_3(CO)_{12}$ or $Fe_3(CO)_9$ was sublimed onto HNa–Y, the zeolite became pink, the characteristic color of the anionic hydride $[HFe_3(CO)_{11}]^-$. Since the adsorption of $Fe_3(CO)_{12}$ proceeds much more slowly, Iwamoto et al. took this as evidence that the anion was generated inside the zeolite supercages, the size of $Fe_3(CO)_{12}$ (ca. 1.05 nm × 0.75 nm) being very close to the diameter of the zeolite windows (~0.74 nm).

The infrared band assigned to the bridging carbonyl (at 1645 cm^{-1}) for $[HFe_3(CO)_{11}]^-$ on HNa–Y zeolite is stronger than the weak, broad band observed by Hugues and co-workers for this material on γ-Al_2O_3.[25] $Fe_3(CO)_{12}$ is also more thermally stable on HNa–Y zeolite than on the alumina and magnesia supports. As for $Fe_3(CO)_{12}$ supported on the metal oxides, the infrared band assigned to the bridging carbonyl occurs about 50 cm^{-1} lower than in a nonpolar solvent, and this has been attributed to an interaction between the Al cations and the lone-pair oxygen of the coordinated CO. Although ESR experiments did not detect paramagnetic species in the formation of the anion on alumina or magnesia supports, the radicals $Fe_2(CO)_8^-$, $Fe(CO)_4^-$, and $Fe_3(CO)_{11}^-$ were detected as intermediates in the formation of $[HFe_3(CO)_{11}]^-$,[11,33]

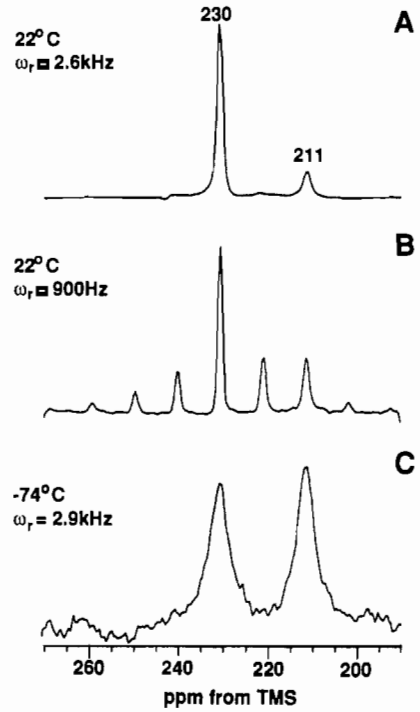

Figure 4. ^{13}C MAS NMR spectra of $Fe_3(CO)_{12}$/HNa–Y zeolite at 8.45 T (90.5 MHz): (A) 22 °C, 2.6-kHz spinning speed, 1000 acquisitions, 2-s recycle time; (B) 22 °C, 900-kHz spinning speed, 500 acquisitions, 2-s recycle time; (C) −74 °C, 2.9-kHz spinning speed, 500 acquisitions, 2-s recycle time.

showing that the zeolite cages stabilize these extremely oxygen-sensitive species.

^{13}C MAS NMR spectra of $Fe_3(CO)_{12}$/HNa–Y zeolite at 90.5 MHz are shown as a function of temperature in Figure 4. At 22 °C, the spectrum contains a small narrow peak at 211 ppm and a large narrow peak at 230 ppm. At very low spinning speeds, sidebands appear for the resonance at 230 ppm, indicating that a small residual chemical shift anisotropy is present (Figure 4B). This residual anisotropy suggests that the motional behavior of the metal carbonyl inside the zeolite cages is more restricted than for a physisorbed species on a metal oxide surface. The small peak at 211 ppm, also observed for the sample on γ-Al_2O_3, is probably due to remaining physisorbed $Fe_3(CO)_{12}$. The resonance at 230 ppm is then, we believe, attributable to an iron carbonyl anion. In contrast to the $Fe_3(CO)_{12}/\gamma$-Al_2O_3 sample, this feature is now very narrow and remains narrow down to much lower temperatures. We show in Figure 4C the ^{13}C MAS NMR spectrum of $Fe_3(CO)_{12}$/HNa–Y zeolite at −74 °C. By −122 °C, the lowest temperature attained, the resonance of the anion has broadened into the baseline, and only the peak due to physisorbed $Fe_3(CO)_{12}$ is visible. The chemical shift of the major species, 230 ppm, is 10 ppm downfield from the isotropic chemical shift of $[HFe_3(CO)_{11}]^-$ in solution. If the surface species is indeed the monoanion, $[HFe_3(CO)_{11}]^-$, this large downfield shift could imply a very strong interaction between the bridging carbonyl and the Al cations or, alternatively, could support the idea that the grafted cluster is fluxional and that all CO's experience an electric field[34] from the zeolite supercage significantly different from that experienced on a planar surface. We now consider these possibilities in more detail.

There have been a number of infrared and ^{13}C NMR spectroscopic studies of the effects of counterions and solvent polarity upon the bridging carbonyl of $[HFe_3(CO)_{11}]^-$.[26-30] Protonation of the bridging carbonyl results in a shift of its ^{13}C NMR resonance, from 283 to 359 ppm. Alkylation of the bridging carbonyl ligand also shifts the resonance downfield, to 357 ppm. The

(33) Iwamoto, M.; Nakamura, S.; Kusano, H.; Kagawa, S. *J. Incl. Phenomen.* **1986**, *4*, 99.

(34) Augspurger, J.; Dykstra, C. E.; Oldfield, E. *J. Am. Chem. Soc.* **1991**, *113*, 2447.

acid–base complex, $HFe_3(CO)_{11}\cdot BF_3^-$, has a bridging carbonyl peak at 355 ppm. These CO–acid interactions involving the bridging carbonyl result in an isotropic chemical shift of ~224 ppm for the completely fluxional anion at room temperature. Thus, the observed isotropic chemical shift of 230 ppm observed for the main surface species observed in the NMR spectrum of $Fe_3(CO)_{12}$/HNa–Y zeolite, although in the right direction, appears to be too large to be due to a strong acid–base interaction between the bridging carbonyl and the zeolite cations. We also expect direct electric field contributions to the isotropic chemical shift from the zeolite supercages to be small, since the lattice charges are fixed while the anion is mobile, so the time average effects will be small. Thus, alternative structures need to be considered.

In another study of the interaction between $Fe_3(CO)_{12}$ and Na–Y zeolites, Ballivet–Tkatchenko et al.[35] adsorbed $Fe_3(CO)_{12}$ onto a dehydrated zeolite. Their infrared spectrum shows only small shifts from the carbonyl frequencies of $Fe_3(CO)_{12}$. After admission of a small amount of water vapor and warming of the sample to 60 °C, additional infrared bands appear. Ballivet–Tkatchenko et al.[35] propose that the following reactions take place in the zeolite when it is hydrated:

$$Fe_3(CO)_{12} \xrightarrow[25\ °C]{Na\text{–}Y/H_2O} [HFe_3(CO)_{11}]^- + CO_2 \qquad (4)$$

$$[HFe_3(CO)_{11}]^- \xrightarrow[60\ °C]{Na\text{–}Y/H_2O} [Fe_3(CO)_{11}]^{2-} \qquad (5)$$

These reactions closely resemble the reactivity of $Fe_3(CO)_{12}$ in basic solution, in which either the monoanion or the dianion forms, depending on basicity.

The dianionic cluster, $[Fe_3(CO)_{11}]^{2-}$, has been studied previously by ^{13}C NMR spectroscopy.[28] The solid-state structure is unusual, with an edge-bridging carbonyl, a highly unsymmetrical face-bridging carbonyl, and nine terminal carbonyls.[36] The infrared spectra of $[Fe_3(CO)_{11}]^{2-}$ in the solid state and solution are very similar, implying that the solution structure also contains an unsymmetric triply bridging carbonyl. However, the ^{13}C NMR spectra show only one sharp singlet, at 230.7 ppm, down to low temperatures, indicating a very small barrier to scrambling between the terminal and bridging sites.[28] This chemical shift is very close to the 230 ppm we observe in Figure 4. Dahl and co-workers[36] discuss the mechanistic pathway of the fluxional behavior of $[Fe_3(CO)_{11}]^{2-}$ in light of the presence of the triply bridging carbonyl ligand and compare it to the proposed mechanism for $[HFe_3(CO)_{11}]^-$. They argue that $[Fe_3(CO)_{11}]^{2-}$ may be regarded as a "defect" structure of $Fe_3(CO)_{12}$ and should thus possess an even lower barrier to carbonyl ligand migration than that (of ≤ 5 kcal mol^{-1}) estimated for $Fe_3(CO)_{12}$. Band and Muetterties[37] predicted facile ligand migration for such "defect" structure clusters, in which there is a departure from the symmetry of the cluster by one metal center, edge or face. This low barrier to ligand migration in $[Fe_3(CO)_{11}]^{2-}$ is in contrast to that of $[HFe_3(CO)_{11}]^-$, where acid–base interactions cause the fluxional processes to stop at higher temperatures. Thus, in addition to the chemical shift of 230 ppm, another important feature in the ^{13}C NMR spectra of $Fe_3(CO)_{12}$/HNa–Y zeolite is that the structure is highly mobile (or presumably fluxional) down to low temperatures. Both observations support a fluxional $[Fe_3(CO)_{11}]^{2-}$ structure for the surface species. In addition, we note that while the 221 ppm resonance assigned to the grafted cluster on γ-Al_2O_3 broadens into the baseline at ~−60 °C and sidebands appear at −80 °C (in the slow-motion regime), the narrow peak at 230 ppm on the zeolite sample only broadens into the baseline at −130 °C. Given all of the above information on model compounds, chemical shifts and fluxional behavior, we believe our results support the idea that the 230 ppm feature arises from the dianion, $[Fe_3(CO)_{11}]^{2-}$, in the zeolite supercages.

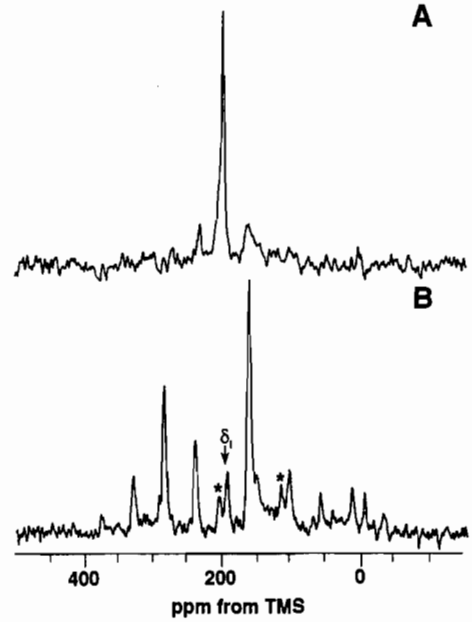

Figure 5. ^{13}C MAS NMR spectra of 2 wt % $Ru_3(CO)_{12}$ on γ-Al_2O_3 at 8.45 T (90.5 MHz): (A) sample spinning under N_2 at 3 kHz, 8036 acquisitions, 2-s recycle time, background subtraction to eliminate the broad ^{13}C background signal from Kel-F in the probe; (B) air-exposed sample, 3-kHz spinning speed, 20 716 acquisitions, 2-s recycle delay.

$Ru_3(CO)_{12}$ Adsorbed on γ-Al_2O_3. The chemisorption of $Ru_3(CO)_{12}$ on alumina, silica, and magnesia has been studied by temperature-programmed decomposition and by IR, Raman, and EXAFS spectroscopies. Although the surface chemistry of $Ru_3(CO)_{12}$ on silica is believed to be very similar to that of $Os_3(CO)_{12}$, the characterization of the surface intermediates has been more difficult, since ruthenium is usually kinetically more reactive than osmium. Whereas the grafted cluster formed when $Os_3(CO)_{12}$ is chemisorbed on silica is air stable, the initial surface species generated when $Ru_3(CO)_{12}$ is chemisorbed on silica is very oxygen sensitive. $Fe_3(CO)_{12}$ is even more reactive on silica, and the oxidized carbonyl species are not sufficiently stable to be characterized. Nevertheless, there have been several studies concerning the catalytic properties of supported ruthenium carbonyls, since ruthenium catalysts are very active for olefin isomerization and hydrogenation, as well as for CO reduction.

Under anaerobic conditions, $Ru_3(CO)_{12}$ is initially physisorbed on dehydroxylated γ-Al_2O_3.[14,38,39] On hydroxylated alumina, Kuznetsov et al.[38] proposed the generation of ruthenium anions, while other groups observed infrared spectra consistent with physisorbed $Ru_3(CO)_{12}$. Both physisorbed $Ru_3(CO)_{12}$ and the chemisorbed anions decompose upon thermal treatment to give a mixture of oxidized species of the form $Ru^{II}(CO)_n(OAl<)$ (n = 2–4), although it is still debatable whether all these species are present. Upon exposure to air, the physisorbed $Ru_3(CO)_{12}$ is oxidized to $Ru^{II}(CO)_2$ units, together with a possible Ru^{IV}–CO center.[39] In general, however, in the literature there are many conflicting results concerning the surface chemistry of $Ru_3(CO)_{12}$ on hydroxylated alumina.

We show in Figure 5 ^{13}C MASS NMR spectra of $Ru_3(CO)_{12}$ supported on γ-Al_2O_3 under anaerobic conditions (Figure 5A) and in air (Figure 5B). The sample spun under N_2 (Figure 5A) shows a single narrow peak, at 198.6 ppm. This resonance is probably due to physisorbed $Ru_3(CO)_{12}$, since the isotropic chemical shift of $Ru_3(CO)_{12}$ in solution is 199.7 ppm. Some groups have proposed the formation of $[HRu_3(CO)_{11}]^-$ on hydroxylated γ-Al_2O_3.[38] The chemical shift of this anion is 200.9 ppm, only slightly downfield from the neutral cluster. Under cross-polarization conditions, only a small peak at 162 ppm is seen, which is observed in most of the oxide-supported metal carbonyl samples

(35) Ballivet-Tkatchenko, D.; Coudurier, G.; Duc Chau, N. In *Metal Microstructures in Zeolites*; Jacobs, P. A., Jaeger, N. I., Jirů, P., Schulz-Ekloff, G., Eds.; Elsevier: Amsterdam, 1982 p. 123.
(36) Yip-Kwai Lo, F.; Longoni, G.; Chini, P.; Lower, L. D.; Dahl, L. F. *J. Am. Chem. Soc.* **1980**, *102*, 7691.
(37) Band, E.; Muetterties, E. L. *Chem. Rev.* **1978**, *78*, 639.
(38) Kuznetsov, V. L.; Bell, A. T.; Yermakov, Y. I. *J. Catal.* **1980**, *65*, 374.
(39) Evans, J.; McNulty, G. S. *J. Chem. Soc., Dalton Trans.* **1984**, 1123.

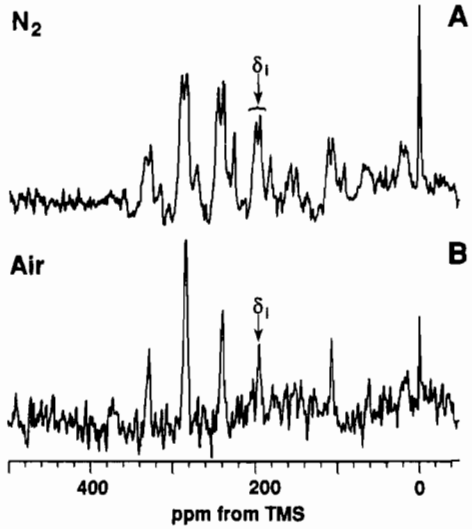

Figure 6. ^{13}C MAS NMR spectra of $Ru_3(CO)_{12}/SiO_2$ at 8.45 T (90.5 MHz): (A) sample spinning under N_2 at 4 kHz, 25 000 acquisitions, 2-s recycle time, 5-ms cross-polarization mixing time; (B) air-exposed sample, 4-kHz spinning speed, 1500 acquisitions, 2-s recycle time, background subtraction to eliminate the ^{13}C Kel-F signal of the probe.

and is due to adsorbed CO_2. This supports the idea that we are observing physisorbed $Ru_3(CO)_{12}$, which is less likely to cross-polarize than the hydrido species. When the sample is oxidized (by switching the spinner gas to air), a series of sidebands centered at 194 ppm appear, which are enhanced by cross polarization. The peak at 162 ppm also increases, due to the formation of more CO_2 as the sample is oxidized. On the basis of the work of Evans and McNulty,[39] the 194 ppm feature is thought to be due to the formation of a dicarbonyl species covalently bonded to the alumina surface, which has restricted motion compared to physisorbed $Ru_3(CO)_{12}$.

$Ru_3(CO)_{12}$ Supported on SiO_2. In the absence of dioxygen, $Ru_3(CO)_{12}$ is initially physisorbed on silica. Upon mild heating (to 70–80 °C), chemisorption occurs, and it is thought that the triruthenium cluster reacts with surface silanol groups.[15,40] The infrared and Raman spectra are very similar to those of the anchored triosmium carbonyl cluster on silica.[41] The oxygen-bridged species $(\mu\text{-H})Ru_3(CO)_{10}(OSi\leftarrow)$ has been characterized by comparing its infrared spectrum with that of the molecular compound $(\mu\text{-H})Ru_3(CO)_{10}(SC_2H_5)$. The surface species is not very stable and is an intermediate in the formation of the surface-oxidized mononuclear carbonyl species $Ru^{II}(CO)_n(OSi\leftarrow)$ ($n = 2, 3$). The di- and tricarbonyl species have likewise been characterized by comparison with the infrared spectra of the model compounds $[Ru(CO)_3Cl_2]_2$ and $Ru(CO)_2Cl_2(py)_2$. The $Os_3(CO)_{12}/SiO_2$ system has been characterized in a similar manner. However, in this case the comparison is more direct, since μ-oxo-bridged triosmium carbonyl clusters, such as $HOs_3(CO)_{10}(-OSiPh_3)$, are available. Quite recently, the results of an EXAFS study of silica-supported $Ru_3(CO)_{12}$ indicated structures in which the ruthenium cluster is bonded to the silica surface by either one bridging or two terminal oxygens.[42] As in the case of the supported osmium clusters, the EXAFS analysis could not distinguish between these two structures but eliminated certain other bonding schemes. When the silica-supported $Ru_3(CO)_{12}$ was exposed to air, the EXAFS spectra were consistent with those of ruthenium dicarbonyl units attached to the surface via Ru–O bonds, with no evidence of Ru–Ru interactions. Previous studies have proposed the presence of an oligomer of a $Ru(CO)_2$ moiety for the air-exposed samples.[39]

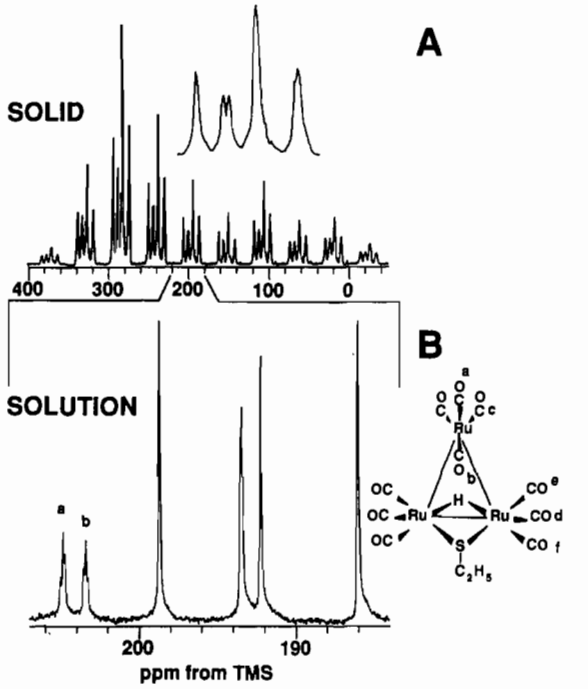

Figure 7. ^{13}C NMR spectra of $[^{13}C]HRu_3(CO)_{10}(SCH_2CH_3)$: (A) solid-state ^{13}C CP-MAS spectrum at 90.5 MHz (4-kHz spinning speed, 500 acquisitions, 15-s recycle time, 50-ms cross-polarization mixing time) the inset expanded region showing the center band; (B) ^{13}C solution spectrum at 125.7 MHz (600 scans, 1-s recycle time).

We show in Figure 6 the ^{13}C MAS NMR spectra of thermally activated $Ru_3(CO)_{12}$ supported on SiO_2, under anaerobic conditions (Figure 6A) and in air (Figure 6B). The sample spun with N_2 (Figure 6A) shows three broad components, having isotropic chemical shifts of 197.7, 192.9, and 179.9 ppm. Upon exposure to air, only the component at 193 ppm remains. Each of these resonances is enhanced under cross polarization, as with the 194 ppm component for $Ru_3(CO)_{12}$ on $\gamma\text{-}Al_2O_3$ shown in Figure 5B. Our sample was prepared under conditions similar to those of the study by Zanderighi et al.[40] These workers found that the grafted cluster, $(\mu\text{-H})Ru_3(CO)_{12}(\mu\text{-OSi}\leftarrow)$ was unstable toward dioxygen, even at room temperature, and was easily oxidized to $Ru(CO)_n(OSi\leftarrow)$ ($n = 2, 3$) in a process facilitated by the presence of water. In decarbonylation/carbonylation processes, the surface equilibrium was found to be strongly shifted toward the dicarbonyl species. Thus, the single component at 193 ppm which remains upon exposure to air is attributed to $Ru(CO)_2(OSi\leftarrow)_2$, basically as found with the $Ru_3(CO)_{12}$ on $\gamma\text{-}Al_2O_3$ system (at 194 ppm). Chemical shift tensor elements for both the 193 and 194 ppm species are given in Table II.

To assist in the assignment of the other two resonances (at 197.7 and 179.9 ppm), the solid-state ^{13}C MAS NMR spectra of the model compounds used in the infrared assignments, $(\mu\text{-H})Ru_3(CO)_{10}(\mu\text{-}SC_2H_5)$ and $[Ru(CO)_3Cl_2]_2$, were obtained. The solid-state and solution spectra of $[^{13}C](\mu\text{-H})Ru_3(CO)_{10}(\mu\text{-}SC_2H_5)$ are shown in Figure 7. As with the $(\mu\text{-H})Os_3(CO)_{10}(CO)_{10}(\mu\text{-OR})$ clusters studied by Walter et al.,[25] six resonances (in a 1:1:2:2:2:2 ratio) are observed in the solution spectra, consistent with C_s symmetry. The two most deshielded resonances are assigned to sites a and b (Figure 7B) on the basis of their relative intensities (but not on a 1:1 basis). These resonances appear as triplets in solution, arising from the overlap of a singlet (one ^{13}C) and a doublet. This doublet is due to ^{13}C–^{13}C J coupling (33 Hz) between the a and b carbonyl sites which are trans across the unique ruthenium atom. In general, $^2J_{CC}$(trans) couplings are typically much larger than $^2J_{CC}$(cis) couplings (1–5 Hz).[43,44] As

(40) Zanderighi, G. M.; Dossi, C.; Ugo, R.; Psaro, R.; Theolier, A.; Choplin, A.; D'Ornelas, L.; Basset, J. M. *J. Organomet. Chem.* **1985**, *296*, 127.
(41) Psaro, R.; Ugo, R.; Zanderighi, G. M.; Besson, B.; Smith, A. K.; Basset, J. M. *J. Organomet. Chem.* **1981**, *213*, 215.
(42) Binsted, N.; Evans, J.; Neville Greaves, G.; Price, R. J. *Organometallics* **1989**, *8*, 613.
(43) Tachikawa, M.; Richter, S. I.; Shapley, J. R. *J. Organomet. Chem.* **1977**, *128*, C9.
(44) Aime, S.; Osella, D. *J. Chem. Soc., Chem. Commun.* **1981**, 300.

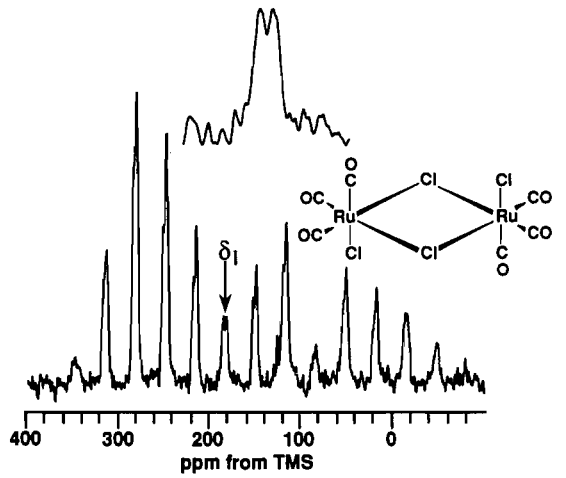

Figure 8. ^{13}C MAS NMR spectrum of $[^{13}C][Ru(CO)_3Cl_2]_2$ at 8.45 T (90.5 MHz; 3.0-kHz spinning speed, 3800 acquisitions, 2-s recycle time), the expanded region showing the center band.

in the case of the $(\mu\text{-H})Os_3(CO)_{10}(\mu\text{-OR})$ clusters, the only other resonance which can be assigned is that of the d site at 193 ppm, which has a large $^2J_{CH}$ coupling since it is trans to the hydride ligand.

The solid-state spectrum of $(\mu\text{-H})Ru_3(CO)_{10}(\mu\text{-}SC_2H_5)$ shows resolution higher than was observed with the analogous oxygen-bridged osmium clusters. However, symmetry-lowering crystal-packing effects still cause the spectrum to be more difficult to interpret than in solution, where there are six resonances (at 204.8, 203.4, 198.7, 193.4, 192.2, and 185.9 ppm, in a 1:1:2:2:2:2 ratio). In the solid state, the solution resonances (at 204.8 and 203.4 ppm) for sites a and b are unresolved, as are those at 192.2 and 193.4 ppm, and instead there are four resonances, at 205, 199, 193, and 185 ppm, in a 1:1:2:1 ratio. The resonances at 199 and 185 ppm, which are singlets in solution, are split into doublets in the solid state, suggesting that the symmetry has been lowered due to crystal-packing effects.

The solid-state spectrum of $[Ru(CO)_3Cl_2]_2$, shown in Figure 8, exhibits a broad resonance centered at about 182 ppm, with a small splitting. In solution, resonances in a 1:2 ratio (at 184.5 and 181.2 ppm) are observed, similar to the spectrum of $[Os(CO)_3Cl_2]_2$.[25] A related compound, $Ru(CO)_4I_2$, has a ^{13}C solution spectrum with resonances at 178.2 and 177.8 ppm.[45]

On the basis of this compilation of chemical shifts and the fact that it disappears upon exposure to air, the resonance observed at 179.9 ppm in the spectrum of $Ru_3(CO)_{12}$ on silica can be assigned either to a tricarbonyl surface species, $Ru^{II}(CO)_3(O\text{–}Si\equiv)_2$, or possibly to the tetracarbonyl $Ru^{II}(CO)_4(OSi)_2$. The resonance at 193 ppm which remains in the air-exposed sample, and which is also observed in the air-exposed $Ru_3(CO)_{12}$ on γ-Al_2O_3, is assigned to the dicarbonyl species. The remaining resonance, at 197.7 ppm, is assigned to the grafted triruthenium carbonyl cluster $(\mu\text{-H})Ru_3(CO)_{12}(\mu\text{-OSi}\equiv)$, on the basis of comparison with the chemical shifts of the molecular cluster $(\mu\text{-H})Ru_3(CO)_{10}(\mu\text{-}SC_2H_5)$ of 205, 199, 193, and 185 ppm. Since the ^{13}C chemical shifts of the oxygen-bridged osmium clusters are 3–5 ppm downfield from those of the thiol derivative,[46] the same could be expected for an oxygen-bridged ruthenium cluster, so it seems very likely that the resonance at 197.7 ppm is in fact due to the grafted cluster.

Recently, a high-resolution ^{13}C MAS study of CO adsorbed on silica-supported metallic Ru particles has been carried out.[47] Duncan et al. observed three resonances, with isotropic shifts of 199, 194, and 178 ppm. These resonances, however, were not separately resolved in their MAS NMR spectra but were inferred from line shape analysis of rotating- and static-sample spectra. These chemical shifts, very close to those observed in our spectra for $Ru_3(CO)_{12}$ on silica, were assigned to multicarbonyl species on isolated Ru atoms and to two types of linearly bonded Ru clusters. However, their resonance at 199 ppm, assigned to the multicarbonyl, was clearly much narrower than the 197.7 ppm resonance observed in our spectrum. Duncan et al. assigned their peak to a dicarbonyl species undergoing motional averaging. The observation of resonances at 194 and 178 ppm, assigned to linearly bonded CO, raises the possibility that these species are also present in our samples, prepared from $Ru_3(CO)_{12}$. However, under the conditions used in our preparation, no evidence for linearly bonded CO has been reported in the infrared and EXAFS data, which support the presence of di- and tricarbonyl species.

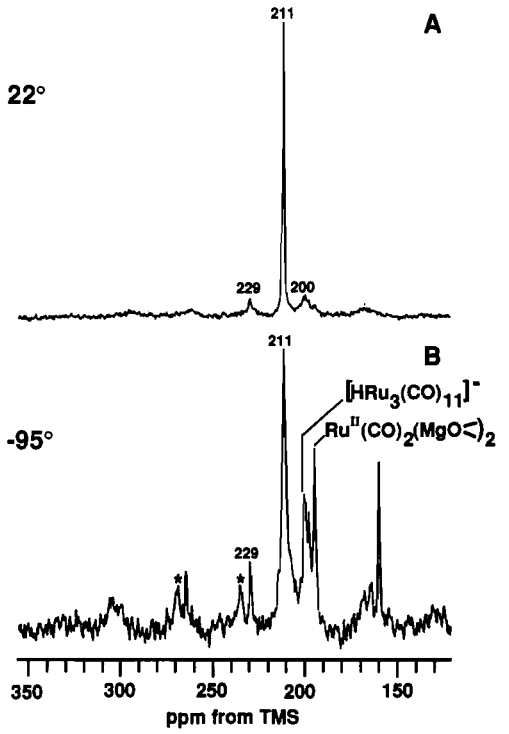

Figure 9. ^{13}C MAS NMR spectra of $Ru_3(CO)_{12}/MgO$ at 8.45 T (90.5 MHz): (A) 22 °C, spinning under N_2 at 3.0 kHz, 2700 acquisitions, 2-s recycle time; (B) −95 °C, spinning under air at 3.2 kHz, 720 acquisitions, 2-s recycle time.

In summary, the ^{13}C MAS NMR spectrum of thermally activated $Ru_3(CO)_{12}$ on silica is consistent with the presence of the surface species previously characterized by IR and EXAFS spectroscopies. These resonances, which are enhanced by cross polarization and display a large chemical shift anisotropy, indicate restricted motion of a species anchored to the surface by covalent bonds. Both the alumina- and silica-supported $Ru_3(CO)_{12}$ samples, when exposed to air, display a single component having an isotropic ^{13}C NMR chemical shift of 193 ppm, which we assign to $Ru^{II}(CO)_2(O\text{–}M\equiv)_2$.

$Ru_3(CO)_{12}$ on MgO. Only a few studies concerning the behavior of $Ru_3(CO)_{12}$ on magnesia have been reported. In one study, Pierantozzi reported the formation of a mixture of anions, $[HRu_3(CO)_{11}]^-$ and $[Ru_6(CO)_{18}]^{2-}$, on hydroxylated magnesia.[16] The surface anions were characterized by infrared spectroscopy and extracted by cation exchange with a solution of $[N(PPh_3)_2]Cl$. In another study, by D'Ornelas and co-workers,[48] only the monoanion $[HRu_3(CO)_{11}]^-$ was observed to form on the surfaces of fully and partially hydroxylated magnesia. This cluster was also characterized by infrared spectroscopy and extraction by cation exchange, as well as by ^1H NMR spectroscopy. Although this behavior of $Ru_3(CO)_{12}$ on magnesia is similar to that of $Fe_3(CO)_{12}$ on alumina or magnesia, the large shift of the bridging ν(CO)

(45) Vancea, L.; Graham, W. A. G. *J. Organomet. Chem.* **1977**, *134*, 219.
(46) Bryan, E. G.; Forster, A.; Johnson, B. F. G.; Lewis, J.; Matheson, T. W. *J. Chem. Soc., Dalton Trans.* **1978**, 196.
(47) Duncan, T. M.; Zilm, K. W.; Hamilton, D. M.; Root, T. W. *J. Phys. Chem.* **1989**, *93*, 2583.
(48) D'Ornelas, L.; Theolier, A.; Choplin, A.; Basset, J. M. *Inorg. Chem.* **1988**, *27*, 1261.

IR band to lower frequency, due to the formation of a tight ion pair with the surface cations, was not observed for the supported $[HRu_3(CO)_{11}]^-$. Instead, the ν(CO) band of the bridging carbonyl of $[HRu_3(CO)_{11}]^-$ on magnesia was the same as that observed in solution.

In Figure 9, we show the ^{13}C MAS NMR spectra of $Ru_3(CO)_{12}$ adsorbed on hydroxylated magnesia. At room temperature (Figure 9A) there are three features: an intense narrow resonance at 211 ppm, a smaller narrow resonance at 229 ppm, and a very weak broad feature at ~200 ppm. The broad component at ~200 ppm cross-polarizes more efficiently than the narrow resonances at 211 and 229 ppm. A variable-temperature MAS NMR study (data not shown) indicates that the narrow peak at 211 ppm is only beginning to broaden by −122 °C, the lowest temperature attained. The broad resonance narrows at lower temperatures (−95 °C, Figure 9B), revealing two sets of sideband patterns, having isotropic shifts of ~199 and 193 ppm.

From the ^{13}C solution chemical shifts listed in Table II for a number of ruthenium carbonyl compounds, the narrow resonances at 211 and 229 ppm can be assigned to the hexaruthenium anions $[Ru_6(CO)_{18}]^{2-}$ and $[Ru_6(CO)_{17}]^{4-}$, respectively, with the 229 ppm feature also possibly containing a contribution from $[Ru_6(CO)_{16}]^{6-}$. The ^{13}C NMR solution spectrum of $[Ru_6(CO)_{18}]^{2-}$, a cluster which possesses both edge- and face-bridging carbonyl groups, remains a sharp singlet down to −100 °C.[49] The small broad resonance at 193 ppm is due to a small amount of the oxidized ruthenium species observed previously ($Ru^{II}(CO)_2(MgO\lessdot)$), and the other broad, weak resonance at 199 ppm may be due to a small amount of the anion $[HRu_3(CO)_{11}]^-$, which has resonances in this region.[50,51] In solution, $[HRu_3(CO)_{11}]^-$ is fluxional at room temperature, with a single resonance at 200.9 ppm, but freezes out at a much higher temperature than the dianion, $[Ru_6(CO)_{18}]^{2-}$. At −50 °C separate peaks appear for the different carbonyl groups, and the anion is totally rigid by −116 °C, whereas the singlet at 211 ppm in a solution of the dianion, $[Ru_6(CO)_{18}]^{2-}$, has not even begun to broaden at this temperature, supporting our assignments.

As discussed above, D'Ornelas and co-workers observed the exclusive formation of the anionic hydride $[HRu_3(CO)_{11}]^-$ on hydroxylated magnesia, whereas Pierantozzi et al. reported the formation of a mixture of the anions $[HRu_3(CO)_{11}]^-$ and $[Ru_6(CO)_{18}]^{2-}$, with the hexaruthenium species being the major product. The formation of the hexaruthenium anion by reaction of $Ru_3(CO)_{12}$ with the basic hydroxyl groups on MgO parallels the chemistry of $Ru_3(CO)_{12}$ in basic solution, in which the anionic hydride $[HRu_3(CO)_{11}]^-$ is initially formed, and after longer reaction times, $[Ru_6(CO)_{18}]^{2-}$ is produced:[52]

$$Ru_3(CO)_{12} \xrightarrow[MeOH]{KOH} [HRu_3(CO)_{11}]^- + CO_2 \quad (6)$$

$$Ru_3(CO)_{12} \xrightarrow[H_2O]{KOH} [Ru_6(CO)_{18}]^{2-} \quad (7)$$

$[Ru_6(CO)_{17}]^{2-}$ is produced by reduction of $[Ru_6(CO)_{18}]^{2-}$, and the isolated salt, while highly air sensitive, is stable at room temperature under a nitrogen atmosphere.[53]

The main difference in the preparation of the magnesia-supported $Ru_3(CO)_{12}$ sample described by D'Ornelas and Pierantozzi groups was the initial treatment of MgO. D'Ornelas and co-workers pretreated the magnesia support with several cycles of oxygen and vacuum at 400 °C to eliminate surface carbonates and then rehydrated with water vapor. Pierantozzi et al. merely dried the MgO at 200 °C under vacuum before impregnation. In addition, the surface area of the MgO used by Pierantozzi et al. was much lower, ~29 m^2/g, versus ~200 m^2/g. Our preparation was similar to that of Pierantozzi et al., except our MgO had a higher surface area. However, higher loadings of $Ru_3(CO)_{12}$ were necessary in order to obtain acceptable signal-to-noise ratios. We used a loading of 4.7 wt % $Ru_3(CO)_{12}$, while D'Ornelas et al. used 2.2%, and our sample was stored for up to 2 weeks before NMR analysis, while the infrared studies of D'Ornelas were done in situ. The higher surface loadings and the longer reaction times may thus be responsible for the formation of $[Ru_6(CO)_{18}]^{2-}$ as the major surface species in our samples. The formation of high-nuclearity clusters under mild conditions on oxide surfaces has also been observed for osmium carbonyls on MgO,[54] as well as for other supported metal carbonyls, such as $[Ru(CO)_3Cl_2]_2$ on Al_2O_3, which reacts with CO to form the triruthenium cluster $[HRu_3(CO)_{11}]^-$.[55]

Conclusions

The results we have presented in this publication indicate that ^{13}C MAS NMR spectroscopy is a potentially useful technique for investigating the mobility, or fluxionality, of metal carbonyl clusters supported on metal oxide (and zeolite) surfaces, but it also clearly points out that definitive characterization of the structures of such species by ^{13}C NMR methods alone is a difficult matter. Some of the reasons are that spectral signal-to-noise ratios are in general low, due to long spin–lattice relaxation times, overall spectral widths are large, due to large CSA values, and individual line widths are often considerable, due to the presence of chemical shift heterogeneity, as well as in some cases extensive line broadening due to chemical exchange at intermediate rates. In addition, more often than not, cross-polarization methods are ineffective, either due to a lack of hydrido groups in the carbonylate, a lack of H–H interactions (which permit efficient cross polarization), long distances to surface hydrogens, or rapid internal or overall molecular motions, which average the C–H dipolar interactions.

On a more positive side, our results give clear evidence for the fluxional nature of the iron carbonylates on γ-Al_2O_3 and HNa–Y zeolite. Comparison of the NMR results for $Fe_3(CO)_{12}$ supported on these two surfaces with its fluxional and chemical shift behavior in various solvents indicates the relative strengths of the acid–base interactions with these supports, as well as assists in identifying the different carbonyl species generated. In addition, our results give evidence for rigid monomer as well as highly fluxional Ru_6 cluster units for $Ru_3(CO)_{12}$ grafted onto γ-Al_2O_3, SiO_2, and MgO.

Acknowledgment. We thank J. Jonas for use of his BET-isotherm apparatus.

Registry No. $Fe_3(CO)_{12}$, 17685-52-8; $Ru_3(CO)_{12}$, 15243-33-1; Al_2O_3, 1344-28-1; SiO_2, 7631-86-9; MgO, 1309-48-4; $(\mu$-H)$Ru_3(CO)_{10}(SC_2H_5)$, 23733-20-2; $[Ru(CO)_3Cl_2]_2$, 22594-69-0; $[HFe_3(CO)_{11}]^-$, 55188-22-2; $[Me_4N][HFe_3(CO)_{11}]$, 33479-90-2; $[Ru_6(CO)_{18}]^{2-}$, 62449-05-2; $[Ru_6(CO)_{17}]^{4-}$, 95828-26-5; $[Fe_3(CO)_{11}]^{2-}$, 25463-34-7.

(49) Johnson, B. F. G.; Benfield, R. E. In *Transition Metal Clusters*; Johnson, B. F. G., Ed.; Wiley: London, 1980; p 526.
(50) Johnson, B. F. G.; Lewis, J.; Raithby, P. R.; Süss, G. *J. Chem. Soc., Dalton Trans.* **1979**, 1356.
(51) Bhattacharyya, A. A.; Nagel, C. C.; Shore, S. G. *Organometallics* **1983**, *2*, 1187.
(52) Eady, C. R.; Jackson, P. F.; Johnson, B. F. G.; Lewis, J.; Malatesta, M. C.; McPartlin, M.; Nelson, W. J. H. *J. Chem. Soc., Dalton Trans.* **1980**, 383.
(53) Bhattacharyya, A. A.; Shore, S. G. *Organometallics* **1983**, *2*, 1251.
(54) Lamb, H. H.; Gates, B. C. *J. Am. Chem. Soc.* **1986**, *108*, 81.
(55) Bergmeister, J. J., III; Hanson, B. E. *J. Organomet. Chem.* **1988**, *352*, 367.
(56) Forster, A.; Johnson, B. F. G.; Lewis, J.; Matheson, T. W.; Robinson, B. H.; Jackson, W. G. *J. Chem. Soc., Chem. Commun.* **1974**, 1042.
(57) Aime, S.; Milone, L.; Osella, D.; Sappa, E. *Inorg. Chim. Acta* **1978**, *29*, L211.
(58) Inkrott, K. E.; Shore, S. G. *Inorg. Chem.* **1979**, *18*, 2817.
(59) Bradley, J. S.; Ansell, G. B.; Hill, E. W. *J. Organomet. Chem.* **1980**, *184*, C33.